Coffee bean particle motion in a rotating drum measured using Positron Emission Particle Tracking (PEPT)

Al-Shemmeri, Mark; Windows-Yule, Kit; Lopez-Quiroga, Estefania; Fryer, Peter J

DOI:
10.1016/j.foodres.2022.112253

Food Research International 163 (2023) 112253

Contents lists available at ScienceDirect

Food Research International

journal homepage: www.elsevier.com/locate/foodres

Coffee bean particle motion in a rotating drum measured using Positron Emission Particle Tracking (PEPT)

Mark Al-Shemmeri [a,b], Kit Windows-Yule [a], Estefania Lopez-Quiroga [a,*], Peter J. Fryer [a]

[a] *School of Chemical Engineering, University of Birmingham, B15 2TT, UK*
[b] *Jacobs Douwe Egberts, R&D Offices, OX16 2QU, UK*

A R T I C L E I N F O

Keywords:
Positron Emission Particle Tracking, PEPT
Drum roaster
Coffee roasting
Particle dynamics

A B S T R A C T

Physicochemical transformation of coffee during roasting depends on the applied time–temperature profile (i.e., rate of heat transfer), with heat transfer phenomena governed by particle dynamics. Positron Emission Particle Tracking (PEPT), a non-invasive imaging technique, was used here to characterise the granular flow of coffee in a real, pilot-scale rotating drum roaster. The experimental study established the impact of drum speed, batch size and bean density (i.e., roast degree) on the system's particle dynamics. Particle motion data revealed two distinct regions: (i) a disperse (low occupancy, high velocity) region of in-flight particles and (ii) a dense (high occupancy, low velocity) bean bed. Implications of these results for heat transfer suggest that controlling drum speed for different density coffees will provide roaster operators with a tool to modulate conductive heat transfer from the heated drum to the bean bed. These comprehensive data thus inform roasting best practices and support the development of physics-driven models coupling heat and mass transfer to particle dynamics.

1. Introduction

During coffee roasting, green (unroasted) coffee is physicochemically transformed (with significant changes in moisture content, chemical composition and microstructure) via the application of specific time–temperature roasting profiles (i.e., rates of heat transfer) (Alessandrini, Romani, Pinnavaia, & Rosa, 2008; Münchow, Alstrup, Steen, & Giacalone, 2020; Pittia, Dalla Rosa, & Lerici, 2001; Romani, Cevoli, Fabbri, Alessandrini, & Dalla Rosa, 2012). It's important to understand the dynamics of particle flow in roasters, as the interactions between coffee beans and heating air, as well as the heated drum wall, are critical to roasting kinetics. The most relevant transient coffee properties are decreasing moisture and mass, and an increasing volume that yields a significant reduction in coffee density.

Roasting is carried out in equipment with a variety of different designs: i.e., rotating drum roasters, tangential (paddle) roasters and spouted (or fluid) bed roasters (Schenker & Rothgeb, 2017). Temperatures in the roasting chamber depend on roaster design and capacity, but typically range 200–300 °C. Spouted (or fluid) bed and tangential (paddle) roasters operate at the higher end of this range, drum roasters operate at the lower end. In the spouted bed roaster, heated air propels a spout of beans into the air that then falls back into a slow-moving bed; heat transfer in the spouting region will be most rapid both because of the high heat transfer coefficients between air and beans, and the high temperature of the air (Brown & Lattimer, 2013). In contrast, for drum roasters (where the drum wall is heated via gas burners, or electric induction heaters), beans are lofted via drum wall lifting and experience high convective heat transfer (for short periods of time), whilst beans near the drum wall will be subject to higher conductive heat transfer (for greater periods of time). In both cases, manipulation of process parameters such as air temperature (or burner gas flow), airflow, drum rotation speed, batch size and roast time will enable the optimisation of the heat transfer rates during roasting and allow roasters to control (and minimise) roast defects and batch homogeneity (Alstrup, Petersen, Larsen, & Münchow, 2020; Gancarz et al., 2022; Giacalone et al., 2019; Hoos, 2015; Rao, 2020; Schenker & Rothgeb, 2017).

Commercially, understanding the interactions between roasting conditions and coffee properties support development of both process and product quality. By establishing bean bed dynamics as a function of both process parameters and product properties, physics-driven models can improve the accuracy and validity of heat and mass transfer simulations that promote virtualisation of the process.

In previous work (Al-Shemmeri, Windows-Yule, Lopez-Quiroga, & Fryer, 2021) we have studied the dynamics of a spouted bed roaster;

* Corresponding author.
E-mail address: e.lopez-quiroga@bham.ac.uk (E. Lopez-Quiroga).

https://doi.org/10.1016/j.foodres.2022.112253
Received 5 September 2022; Received in revised form 18 November 2022; Accepted 26 November 2022
Available online 29 November 2022

here, a similar approach is applied instead to the case of drum roasters, a distinct but similarly widely used geometry (González, Windows-Yule, Luding, Parker, & Thornton, 2015; Henein, Brimacombe, & Watkinson, 1983; Mellmann, 2001).

1.1. Particle-fluid interactions

Coffee development during roasting depends on the heat transfer mechanisms, and their relative rates, which are governed by the system particle dynamics. Coupling of particle–particle, particle–wall and particle–fluid interactions through empirical investigations and simulations will provide a comprehensive understanding of the process.

Several studies have used Computational Fluid Dynamics (CFD) to model flow behaviour in dilute granular systems - such as Alonso-Torres, Hernández-Pérez, Sierra-Espinoza, Schenker, and Yeretzian (2013), Chiang, Wu, & Kang, (2017), Oliveros, Hernández, Sierra-Espinosa, Guardián-Tapia, and Pliego-Solórzano (2017) and Abdul Ghani, Bingol, Li, Yu, and Young (2019). Ma, Zhou, Liu, Chen, Xia, and Zhao (2022) recently reviewed methods to successfully couple CFD and Discrete Element Method (DEM) simulations of non-spherical particles. Although difficult to validate, CFD-DEM simulations can determine both lumped and distributed temperature distributions within spouted bed roasters (Azmir, Hou, & Yu, 2020; Bruchmüller, Gu, Luo, & Van Wachem, 2010; Machado, Resende, Lima, Brandão, Pivello, Nascimento, & Duarte, 2018). Che et al., (2023) presented a CFD-DEM model using a spouted bed coffee roaster as a case study. The CFD-DEM model was calibrated using PEPT data (Al-Shemmeri et al., 2021), with model parameters and drag coefficients optimised to accurately capture particle recirculation times, occupancy and velocity profiles, and regional mass fractions.

Granular flow in rotating drums with simplified geometries (i.e., no baffles or vanes) (González et al., 2015; Henein et al., 1983; Mellmann, 2001), and/or with simple (often monodispersed) particle shapes (Ding, Forster, Seville, & Parker, 2002; Govender, 2016; Lim, Davidson, Forster, Parker, Scott, & Seville, 2003; Morrison, Govender, Mainza, & Parker, 2016; Pathmathas, 2015; Windows-Yule et al., 2016, 2017) has been well documented. Granular systems of polydisperse, aspherical particles in rotating drums with internally mounted vanes are less understood.

Particle motion can be characterised into several regimes: of relevance here are rolling, cascading and cataracting motions (Henein et al., 1983; Mellmann, 2001). The Froude number, a dimensionless number describing the ratio of inertial (i.e., centripetal) and gravitational forces, is often used to define particle dynamics and characterise the flow regime in granular systems (Arntz et al., 2008; Henein et al., 1983; Mellmann, 2001). Jones et al., (2022)studied the motion of fabrics in tumble dryers using PEPT and found that both the axial and radial displacement of particles were determined by load size. Jones et al., (2022) used an effective Froude number to characterise particle behaviour relative to the drum wall – this approach is suitable for aspherical particles (i.e., coffee beans). The impact of particle density, batch size (i.e., fill volume) and drum rotation speed on Froude number are considered here in detail.

In coffee literature, empirical studies are limited to imaging of transparent model systems, where accuracy is low and restricted to two-dimensional analysis. Cristo, Martins, Oliveira, and Franca (2006) and Resende, Machado, Duarte, and Barrozo (2017) used image analysis of transparent model drums to visualise the dynamic behaviour of coffee in rotating drums. Proposed empirical models predicted the optimal rotational speed to maximise mixing in the roaster and hence improve heat transfer (Cristo et al., 2006; Resende et al., 2017).

1.2. Positron Emission Particle Tracking (PEPT)

Positron Emission Particle Tracking (PEPT) is an imaging technique used to characterise particle motion in particulate and multiphase systems. For particles labelled with positron-emitting radioisotopes, Lagrangian trajectories can be captured in three-dimensions with high temporal and spatial resolution (Windows-Yule et al., 2020, 2022a). PEPT measurements rely on the ergodic assumption (Wildman, Huntley, Hansen, Parker, & Allen, 2000): for steady-state systems, time-averaged behaviour exhibited by a single particle in a homogenous system is assumed representative of the ensemble-averaged behaviour of all particles in the system. Development of the PEPT method was comprehensively detailed by Parker, Broadbent, Fowles, Hawkesworth, and McNeil (1993) and Parker (2017), with best practices and applications reviewed by Windows-Yule, Seville et al. (2020). Recent PEPT studies (Nicuşan & Windows-Yule, 2020; Al-Shemmeri et al. 2021; Jones et al., 2022) have established a framework for post-processing and analysis of PEPT data that will be employed here. This enables the location of tracer particles, identification of Lagrangian trajectories and conversion to Eulerian data, with subsequent visualisation tools developed based on the established framework. Full details regarding PEPT may be found in (Windows-Yule, Nicuşan, Herald, & Manger, 2022b).

This study aims to (i) gain insight into the dynamics of aspherical coffee beans within the roaster subject to different process conditions and (ii) establish data to be used as accurate, dynamic boundary conditions suitable for coupling with heat and mass transfer simulations. From these fully quantitative (and three-dimensional) time-stamped Cartesian coordinates, the residence time and velocity of particles can be extracted. The residence times in different regions can be used as the simulation's time step, whilst particle velocities can be used in correlations to estimate the regional heat transfer coefficients.

As coffee roasting occurs over much shorter timescales than those required for PEPT measurements, particle dynamics corresponding to different stages of real roasting will be inferred through the study of coffee with different roast degrees and densities (thus emulating physicochemical changes that occur during roasting).

2. Materials and methods

2.1. Coffee beans

Before PEPT measurements, batches of Kenyan Arabica coffee were roasted in a spouted bed roaster with a constant inlet air temperature of 250 °C as detailed by Al-Shemmeri et al. (2021). Roast time was varied to obtain green (unroasted, i.e., roast time, t = 0 s), part-roasted (t = 138 s) and roasted (t = 278 s) coffee samples – corresponding to whole bean (surface) colours of 42, 50 and 70 for green, part-roasted and fully-roasted coffees (R100B, ColorTrack. Fresh Roast Systems). The density of these samples is representative of coffee, independent of the roaster used in preparation of the samples and were used to compare particle dynamics with those documented by Al-Shemmeri et al. (2021).

Intrinsic density was determined by measuring the coffee bean principal dimensions (digital calipers, IP54, Perciva) and mass (XSR204, Mettler-Toledo) of 25 beans from each sample set. From bean dimensions, a (width), b (depth) and c (length) (mm), bean volume, V_b (mm^3) was calculated assuming the bean is hemi-ellipsoidal ($V_b \approx \frac{\pi abc}{6}$). Bulk density was calculated from the measured mass (Lunar balance, Acaia) of coffee that occupies a 250 ml beaker, where beans settled freely. The top of the beaker was smoothed to ensure a level fill and measurements were repeated in triplicate using aliquots of each sample set. Packing density (i.e., number of beans per unit mass (kg^{-1}) was calculated from the measured mass of 25 coffee beans, performed in triplicate. Coffee properties are detailed in Table 1.

2.2. Coffee roaster

A pilot-scale rotating drum roaster (Bullet R1 V2, Aillio) was used for the flow studies. The roasting chamber has a diameter of 160 mm, with a depth of 295 mm. The roaster, rotating clockwise in xy, employs 3

Table 1
Properties of Kenyan Arabica coffee beans of different roasting degrees.

Coffee Sample	Roast Time (s)	Roast Loss (%)	Principal Dimension a (mm)	Principal Dimension b (mm)	Principal Dimension c (mm)	Volume (mm^3)	Intrinsic Density (kg m^{-3})	Bulk Density (kg m^{-3})	Packing Density (kg^{-1})
Green	0	0.0	6.11 ± 0.39	3.95 ± 0.48	8.36 ± 0.93	106.0 ± 20.2	1279.4 ± 86.5	705 ± 11	7420 ± 280
Part-Roasted	138	8.1	7.05 ± 0.52	4.61 ± 0.56	8.82 ± 0.86	151.0 ± 30.7	805.8 ± 110.7	460 ± 9	8373 ± 499
Roasted	278	16.6	7.49 ± 0.54	4.91 ± 0.53	9.97 ± 1.07	192.9 ± 37.8	563.4 ± 51.4	301 ± 6	9250 ± 326

internal vanes (shown in Fig. 1(b-e)) to: (i) promote bean lift in the bottom left region of the roaster (in *xy*), (ii) improve axial mixing (in *z*) and (iii) positively displace the beans toward the front face (in *xy*) (necessary to remove coffee after roasting).

2.3. Process parameters and conditions

In drum roasters, both drum rotation speed and batch size influence particle dynamics. Here, three different batch sizes (300 g, 600 g, 900 g) as well as three different drum rotation speeds (42 rpm, 56 rpm, 78 rpm) were chosen to emulate roasting conditions through the study of coffee beans of different roast degrees (i.e., green, part-roasted and roasted)

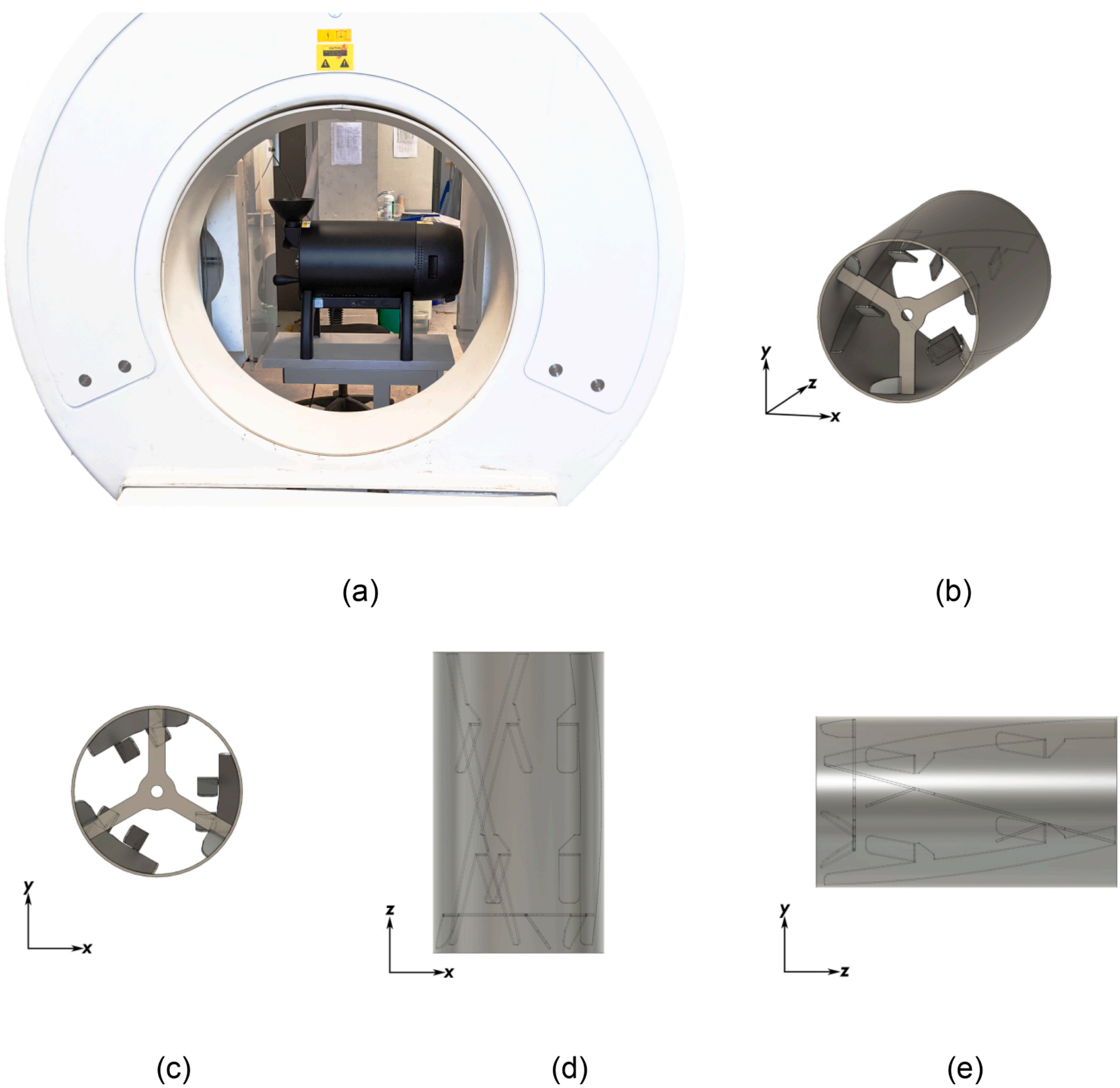

Fig. 1. The rotating drum roaster (a) in the ADAC forte scanner, alongside a simplified schematic of the roasting chamber and established orientation of system for (b) x,y,z (c) x,y (d) x,z (e) z,y. STEP file provided by Aillio.

and to reflect realistic variations of process parameters that a roaster might employ. The experimental design consisted of five process conditions (300 g at 42 rpm, 300 g at 78 rpm, 600 g at 56 rpm, 900 g at 42 rpm and 900 g at 78 rpm) for each coffee sample (green, part-roasted and roasted).

The Bullet roaster utilises arbitrary values for drum rotation speed, airflow and power (ranging integers 1–9). For PEPT measurements, the roaster was operated with an airflow setting of 7 (to minimise smoke and chaff accumulation in the roasting chamber during real roasting) and a power setting of 0 (i.e., no heating).

Air velocity was determined at the air outlet (ø 50 mm equivalent pipe diameter) of the roaster using a hot-wire anemometer (405i, Testo). The roaster was operated empty (i.e., with no beans) at ambient temperature (*ca.* 25 °C) for 10 mins at fan settings 1–9. Air velocities at the roaster outlet ranged 0.6–1.6 m s^{-1}.

Air velocity at setting 7 (measured at the roaster outlet) was 1.4 m s^{-1} at ambient temperature (20 °C); within the roasting chamber (ø 160 mm), air velocity was approximately 0.13 m s^{-1}. For elevated temperatures of 220 °C (i.e., +200 °C differential), where air density is 60% lower, a greater air velocity in the roasting chamber was estimated at 0.22 m s^{-1}. As CFD studies (Alonso-Torres et al., 2013) have used air velocities of 2 m s^{-1} to model convective heat transfer over stationary coffee beans, and experimental spouting velocities of coffee beans in a 0.5 kg spouted bed roaster are in the range 4–10 m s^{-1} (Al-Shemmeri et al., 2021), the low airflow (velocity $\ll$ 2 m s^{-1}) employed in this pilot-scale drum roaster is expected to have no impact on particle motion.

The volume occupied by a static bean bed (i.e., coffee beans within the roasting chamber with no applied airflow, or any drum rotation) was determined using the coffee bulk density (Table 1), specified batch size and roaster geometry. The bean bed was assumed uniform in *z* (according to Fig. 1) with a depth of 295 mm. The equivalent area occupied by a static bean bed in *xy* is thus a function of the coffee batch size and bulk density, in addition to the geometry of the roaster. For reference, the roaster has a volume of 5931 cm^3 and a maximum area in *xy* of 201.1 cm^2. Table 2 outlines the static bean bed area according to batch size and coffee density.

2.4. Positron Emission particle Tracking (PEPT)

2.4.1. Experimental setup

The entire system was positioned within the camera most sensitive field of view, thus ensuring maximal acquisition rate and precision (Herald, Wheldon, & Windows-Yule, 2021). Fig. 1(a) shows the roaster positioned within the space between ADAC forte scanner gamma-ray detector heads, whilst Fig. 1(b-e) presents a schematic of the roasting chamber detailing the established system orientation. The centre of the roasting chamber was used as the origin for the data. Further details of the positron camera are given in Parker, Forster, Fowles, and Takhar (2002) and Herald et al. (2021).

Table 2
Static bean bed area of coffee beans as affected by batch size and bean density in plane *xy*.

Coffee Sample	Batch Size (g)	Fill Volume (cm^3)	Fill Percentage (%)	Bed Area in *xy* (cm^2)
Green	300	426	7.2	14.4 ± 0.2
Green	600	851	14.3	28.8 ± 0.4
Green	900	1277	21.5	43.3 ± 0.7
Part-Roasted	300	652	11.0	22.1 ± 0.5
Part-Roasted	600	1304	22.0	44.2 ± 0.9
Part-Roasted	900	1957	33.0	66.3 ± 1.4
Roasted	300	997	16.8	33.7 ± 0.7
Roasted	600	1993	33.6	67.5 ± 1.3
Roasted	900	2990	50.4	101.2 ± 2.0

2.4.2. Tracer labelling

A single coffee bean was selected from each sample set and principal dimensions of the selected particles were checked to be within one standard deviation of the batch mean. Selected particles were indirectly labelled by pipetting 2 ml of water – containing ions of Fluorine-18, a β^+ -emitting radioisotope - onto the particle surface (Parker, 2017). After allowing 30 mins for absorption of irradiated water, the excess of water, which was determined gravimetrically, was removed by drying the particle under a heat lamp. A balance with 0.1 mg precision (XSR204, Mettler-Toledo) was used to measure the bean mass before and after labelling, the two weights agreed to within the stated precision of the balance. The labelled particle was returned to the sample set and placed in the roaster. As the tracer particle is physically identical to its counterparts in the system, measurements can be considered entirely non-invasive.

Experiments were conducted over five consecutive days, with the order of experiments governed by the activity of the labelled tracers on each day. Higher bean densities typically had lower tracer activity, so higher density tracers (i.e., experimental conditions using higher density coffees) were prioritised. For PEPT measurements, the roaster is not heated, and the system is at thermal equilibrium prior to charging with coffee.

2.4.3. PEPT data capture and processing

For the system to be ergodic, data must be captured over a period sufficient for the tracer particle to fully explore the roasting chamber. Thus, once particle motion was established at ambient temperatures (*ca.* 25 °C), data were captured for 60 mins.

Lines of Response (LoRs) were obtained using the positron camera, with positional data determined through implementation of location and trajectory machine-learning algorithms (Nicuşan & Windows-Yule, 2020). The algorithms used to locate the tracer were implemented using PEPT-ML – an open-source Python framework (https://github.com/uob-positron-imaging-centre/pept). PEPT-ML generated time-stamped Cartesian coordinate data for each experimental run. Experimental datasets were segmented to account for systemic variability such that each 60 min experiment generated two 30 mins datasets, subsequently analysed in MATLAB (2020a, MathWorks). All computational work was performed using the BlueBEAR HPC service of the University of Birmingham.

Timestamped Cartesian coordinates were transformed to time-averaged Eulerian flow fields through division of the system volume into uniform elements (pixels in 2D). A mesh of 85x85 elements in 2D was defined, with element dimensions equivalent to the approximate intrinsic spatial resolution of the camera. Spatial accuracy during post-processing of PEPT data is detailed in Windows-Yule et al. (2022b). Here, mesh element dimensions of 3.5x3.5 mm in 2D were used for transformation of Lagrangian trajectories to Eulerian flow fields. For analysis of ergodic systems, allowing sufficient time for data capture and appropriate sizing of mesh element dimensions, the decay of tracer activity (half-life of 109 mins), is assumed to have no significant impact on the measurements.

Eulerian flow fields are determined from the residence time of the tracer in each element (Windows-Yule, Seville, Ingram, & Parker, 2020), and the velocity magnitude of the tracer in each element is expressed as $\sqrt{(v_x^2 + v_y^2)}$ in *xy* and $\sqrt{(v_x^2 + v_y^2 + v_z^2)}$ in *xyz*. Particle velocities are later discussed as the median of velocities calculated at each time step corresponding to the obtained Cartesian data.

Particle displacement was considered here by studying the horizontal (maximum difference in position in *x*) and vertical (maximum difference in position in *y*) distances travelled by the particle during each rotation (Windows-Yule, Seville, Ingram, & Parker, 2020). Single rotation trajectories were segmented based on the timestamped Cartesian coordinates, with each rotation initialising when the tracer crosses the boundary of $y = 0$, when $x < 0$ in the plane *xy* (i.e., when the particle is lifted along the drum wall).

Total occupied area is defined based on the sum of non-zero elements of occupancy profiles in *xy*. Bean bed area was delineated from total occupied area via application of an Otsu method (Otsu, 1979) as detailed in Al-Shemmeri et al., (2021).

Regional mass fractions were determined based on the coffee sample bulk density, roaster geometry and the occupied, regional area estimated from occupancy profiles. For specified process conditions, the total occupied in a given two-dimensional cross-section (A_o), is determined from the number of non-zero elements (n_{nze}) and the elemental area (A_e) of occupancy profiles:

$$A_o = \sum n_{nze} A_e \tag{1}$$

The area occupied by the bean bed (A_{bb}) is calculated using a similar approach. Bean Bed Mass Fraction (BBMF) is determined via the bean bed area, batch size ($m_{b,s}$) and coffee bulk density (ρ_b), assuming that the bed is uniform in the axial (*z*) direction of the roasting chamber (R_d):

$$BBMF = \frac{R_d A_{bb} \rho_b}{m_{b,s}} \tag{2}$$

Changes in regional mass fractions were used to infer dynamic particle behaviours that result from (i) physicochemical transformations (ii) changes in process parameters during roasting.

2.4.4. Drum rotation speed and Froude number

The drum rotation speed was determined via PEPT measurements where a labelled tracer was affixed to the drum in a known location, with the drum operated at rotation settings 1, 5 and 9 at ambient temperatures (*ca.* 20°c) with data captured for 10 mins. Drum rotation speeds corresponding to drum speed set points are outlined in Table 3. LoRs analysis was performed using PEPT-ML, with trajectory analysis performed in MATLAB. During trajectory analysis, the trajectories were segmented each time the particle crossed the boundary of $y = 0$, when $\times < 0$ in the plane *xy*. The rotation speed of the drum was determined as the inverse of the mean cycle time.

Froude number (Fr) is calculated as a function of the angular velocity (ω), drum radius (R) and gravitational acceleration (g) (Henein et al., 1983):

$$Fr = \frac{\omega^2 R}{g} \tag{3}$$

Froude numbers corresponding to rolling and cascading motion are typically expected to fall in the range $10^{-4} < Fr < 10^{-1}$, with the transition from cascading to cataracting motion occurring at $Fr \sim 10^{-1}$ (Mellmann, 2001). Fr at the drum wall (i.e., where $R = r_{drum} = 0.08$ m) was calculated according to Eq. (3) for each drum rotation speed – values are stated in Table 3. To account for particle size – where particle radius (r) is significant relative to the drum radius – Fr becomes (Arntz et al., 2008; Juarez, Chen, & Lueptow, 2011):

$$Fr = \frac{\omega^2 (R - r)}{g} \tag{4}$$

Here, particle Froude numbers were determined for those with positive velocities (i.e., for upward trajectories in the lifting region only) at the boundary of $y = 0$, when $\times < 0$ in *xy* (i.e., the initial point of individual particle trajectories as described in Section 2.4.3).

The internal vanes in the roasting chamber increase drum wall lift and push particles toward the drum front face. Particle angular velocity will be influenced by both the forces induced by the drum, and the lifting force of the vanes. For dense particles and low rotation speeds, particles at the drum wall will show greater Froude numbers than those in the bean bed bulk, where the Fr is approximately equal to that of the drum wall itself (see Table 3 for reference values).

Table 3
Drum rotation speeds determined at set points used for PEPT measurements.

Drum Speed Set Point (au)	Drum Rotation Speed (rpm)	Drum Wall Froude Number, *Fr*
1	42.2 ± 0.3	0.16
5	56.2 ± 0.5	0.28
9	77.7 ± 1.0	0.54

3. Results & discussion

3.1. Types of data obtained

Fig. 2 shows the type of data obtained from PEPT. Typical individual particle trajectories are illustrated in Fig. 2(a), while occupancy and velocity fields are represented in Fig. 2(b) and Fig. 2(c), respectively.

Particle trajectories - illustrated by coloured lines in Fig. 2(a) - show the characteristic behaviour of a rotating drum, with a bed of beans of high density and a region of beans in-flight. From these trajectories both velocity and time spent by a particle in each region (i.e., residence time) can be determined.

Eulerian flow fields are first presented as occupancy profiles (Fig. 2(b)) – where high occupancy regions are red; low occupancy regions are dark blue. Empty regions are absent of data (i.e., particles did not pass through these elements). All is expressed as a fraction of total experimental time; the dense bean bed and low occupancy flight region can be clearly seen. This data can be turned into velocity fields overlaid with particle velocity vectors (Fig. 2(c)) – where high velocity regions are red; low velocity regions are dark blue; arrow size indicates the magnitude of the velocity vector – expressed as the velocity magnitude of the tracer in each element. Again, the slow-moving bed and rapid in-flight region can be seen; the bed contains a region of near-zero flow around which beans rotate.

3.2. Effect of process parameters on particle behaviour

3.2.1. Effect of roasting degree on particle dynamics

Fig. 3(a-c) presents PEPT-obtained Cartesian data, overlayed with individual particle trajectories (in different colours). These plots illustrate particle-level motion of different density coffees in the roasting chamber under the same process conditions (batch size of 900 g and drum rotation speed of 42 rpm). Roasted bean trajectories are significantly more uniform and show rotation about a stationary point, as comparison of trajectories presented in Fig. 3(a) and Fig. 3(b) reveal. Lagrangian trajectories and Eulerian flow fields show two distinct particle behaviours:

(i) particles in the bean bed rotate around the bed centre of mass.

(ii) particles near the drum wall are subject to lifting (either by the drum centrifugal force, or by the vanes), detach in the upper left quadrant of the drum (in plane *xy*) and then free fall through the disperse region (i.e., are in-flight).

Increasing roast degree and bean volume significantly change the behaviour of the system. During roasting, beans lose mass – this affects drum wall lifting. Increasing roast degree increases axial travel distances due to greater centrifugal forces and improved attachment in the upper left region of the drum, similar to phenomena seen by Jones et al., (2022). Changes in roast degree (from green to roasted) decrease the size of the bean bed - see the change in the green/yellow region in Fig. 3(d-f) – and thus increase the occupancy in other regions – i.e., see how the light blue region in Fig. 3(d-f) changes. Readers are referred to Ingram, Seville, Parker, Fan, and Forster (2005) for studies of particle dispersion, and to Ding et al. (2002) for studies of segregation in rotating drums.

3.2.2. Effect of batch size on particle dynamics

The effect of batch size for roasted coffee operated with a drum rotation speed of 42 rpm (shown in Fig. 4) reveals that as batch size increases, the bean bed area (in *xy*) increases but is less densely occupied (Fig. 4(c-d)), not dissimilar to observations of increasing bean volume.

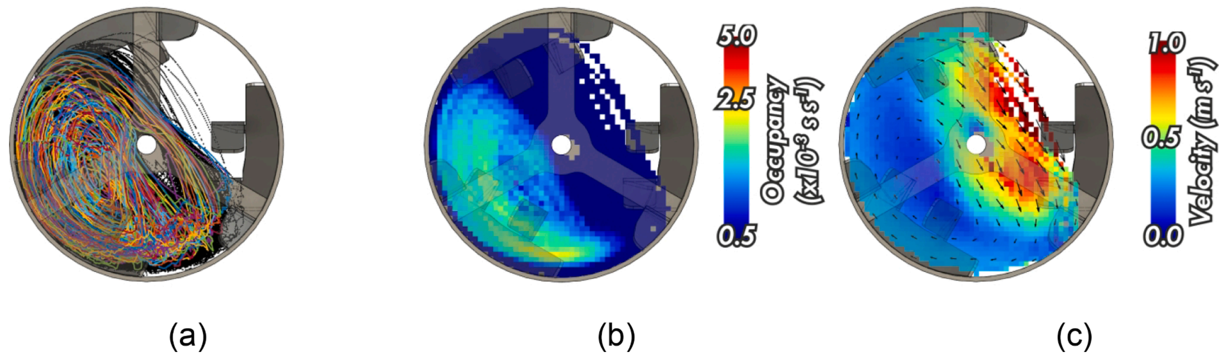

Fig. 2. Visualisation of PEPT data: (a) Cartesian coordinates, overlayed with individual Lagrangian particle trajectories, (b) Eulerian occupancy profile and (c) Eulerian velocity profile. Data corresponds to 30 mins of data for 900 g of roasted coffee with a drum rotation speed of 42 rpm (clockwise).

The corresponding velocity profiles (Fig. 4(e-f)) show that in-flight velocities are greater for lower batch sizes (300 g). Again, the highest batch size shows more uniform rotational behaviour (Fig. 4(a-b)), with the point about which the beans rotate – the centre of the deep blue low velocity region in Fig. 4(e-f) – being closer to centre of the drum.

3.2.3. Effect of drum rotation speed on particle dynamics

Fig. 5 demonstrates the effect of drum rotation speed on particle dynamics for 900 g of part-roasted coffee. Whilst bean bed occupancy has marginally lower at lower rotation speeds (Fig. 5(c-d)), the bean bed area (in *xy*) decreases significantly as drum rotation speed increases due to increasing homogeneity of particle trajectories (Fig. 5(a-b) and centrifugal effects of rotation.

Fig. 5(e-f) shows that in-flight velocities are comparable, although there is a greater fraction of the batch travelling at higher velocities for higher drum rotation speeds. Bean bed velocities also increase as drum rotation speed increases, due to conservation of momentum and an effective no-slip boundary at the wall.

3.3. Analysis across processing conditions – Combined effect of roasting degree, batch size and drum speed

3.3.1. Flow velocities and particle trajectories

Both process parameters and product properties have a significant impact on the occupancy and velocity profiles. Fig. 3(d-i), Fig. 4(c-f) and Fig. 5(c-f) show two distinct regions of occupancy and velocity: (i) a dense bean bed of high solids fraction, where beans move slowly (0.0–0.5 m s^{-1}) and (ii) a disperse in-flight region, where beans travel at higher velocities (0.5–2.0 m s^{-1}). These data (particularly those in Fig. 3) highlight the potential to modulate particle dynamics via simple roasting control strategies – changing the speed of rotation has a clear effect on the bed and in-flight volumes (see Fig. 5), so changing drum rotation speed during processing could be used to account for changes in bean density.

Fig. 6(a) and 6(b) show the variation of particle travel distance (for a single cycle) in vertical and horizontal directions, respectively – data is shown for part-roasted conditions, data for all other roasting degrees across conditions are similar. The vertical distances travelled are *ca.* 0.16 m, i.e., close to the diameter of the roaster, showing the efficiency of the drum vanes, and movement is greater for higher drum rotational velocities. For horizontal travel, the behaviour is bimodal, with peaks *ca.* 0.05–0.08 and 0.12–0.16 m; this probably corresponds to beans in the dense bed and dilute flight regions, demonstrated by the flow fields in Fig. 3(d-e), but not in Fig. 3(f).

For vertical travel distances, the impact of roast degree is most apparent for high drum rotation speeds (78 rpm). Under these conditions, increasing roast degree increases the vertical travel distances due to greater centrifugal forces and improved attachment in the upper left region of the drum.

At low to moderate drum speeds (42–56 rpm), batch size has no significant impact on vertical travel distance (Fig. 6(a)). When green and part-roasted coffees are subject to high drum speeds (78 rpm), smaller batches - with fewer beans in the bed and more in-flight particles - cause beans to travel over greater vertical distances than for larger batches. This phenomenon is not observed for roasted coffee and can be attributed to drum wall lifting – i.e., beans of higher density are more influenced by centrifugal forces at the wall.

For smaller batches of green and part-roasted coffee, motion tends toward cataracting, and particle behaviour becomes more homogenous (i.e., a greater number of particles follow similar trajectories). For roasted coffee at high drum speeds (78 rpm), there is little impact of batch size on both vertical and horizontal travel distances, which might be a result of particle collisions with the drum central axis - this generates a bi-modal distribution of horizontal travel distances (seen in Fig. 6(b) with a local minimum at approximately 0.08 m (the drum radius).

Fig. 6(b) shows that at low drum speeds (42 rpm) all coffees tend to travel horizontal distances less than the drum radius (falling through the in-flight region at $r < R$) during a single rotation. Increasing drum speed increased the vertical travel distance Fig. 6(a), where particles are subject to drum wall lifting. The impact of drum speed on vertical travel distance decreased as particle density decreased. For large batches (900 g), drum rotation speed has little impact on the median horizontal travel distance, but greater drum speeds lead to more particles travelling distances greater than the drum radius (as illustrated by Fig. 6(a-b)). There is no real impact of drum speed on horizontal travel distances for large batches (900 g) of roasted coffee due to the large fill volume, which increases bed volume and causes more beans to follow similar trajectories (i.e., bean behaviour becomes more homogenous).

Velocity (vector in *xyz)* distributions for part-roasted beans are displayed in Fig. 6(e). Particle velocity is governed by the drum rotation speed. The slow-moving core within the bean bed has no real impact on velocity distributions due to the low fraction of the batch that fall into such trajectories. For a specified drum rotation speed, increasing batch size has little influence on the median particle velocity, although it increases the homogeneity of particle behaviour (i.e., decreases the range of particle velocities). Batch homogeneity is critical to most definitions of quality, particular for products sold as whole beans, where large distributions in size and colour (a result of roast defects such as tipping and scorching) are likely to be perceived negatively by consumers (Giacalone et al., 2019). Whilst bean breakage in large roasting systems is a concern (particularly when whole beans are conveyed at high speed to packing lines), in the pilot-scale roaster there was no evidence of bean breakage to suggest process conditions influence the susceptibility to breakage of beans.

3.3.2. System characterisation using Froude number

Froude numbers for particles lifted by the drum wall were calculated

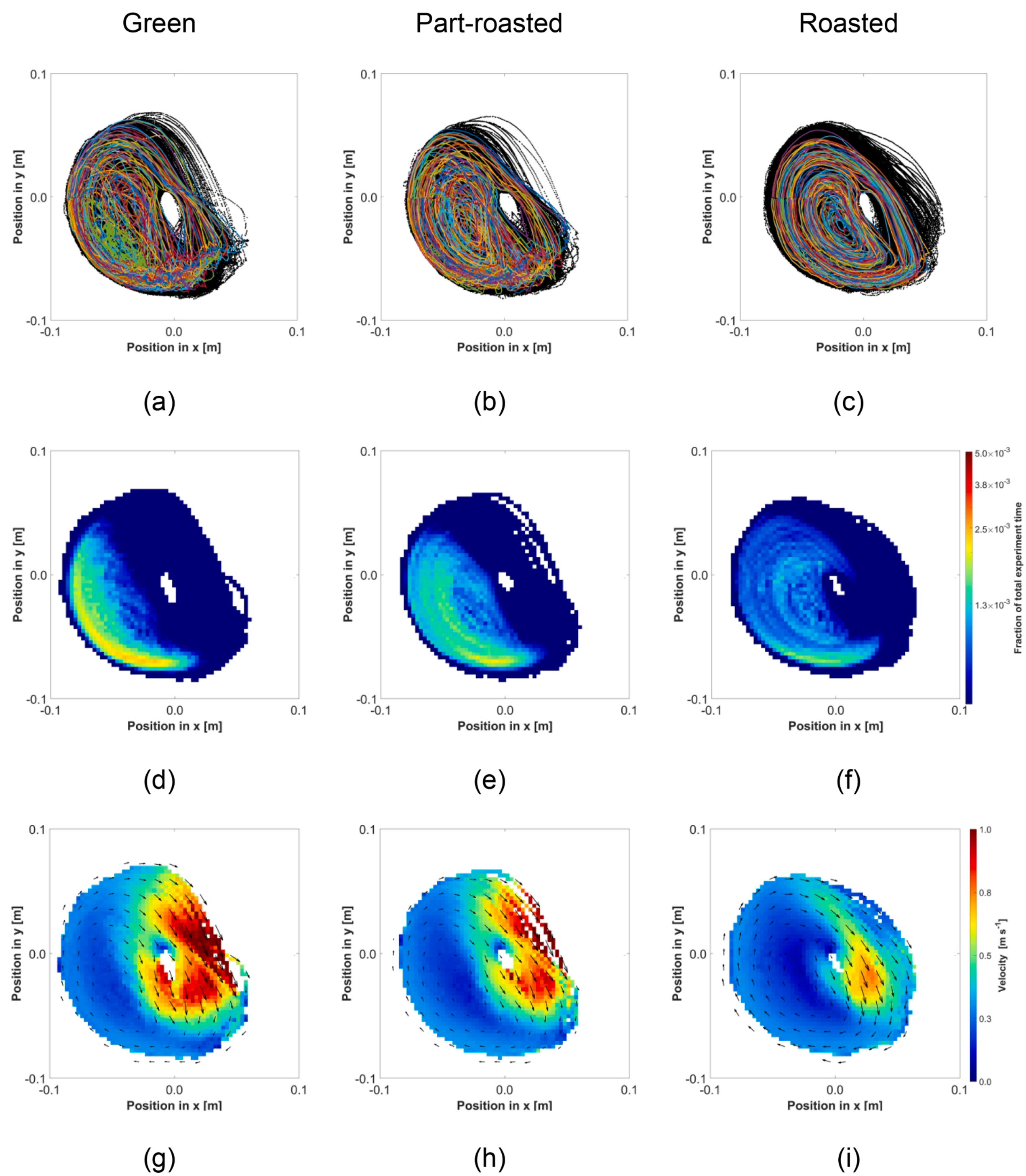

Fig. 3. Experimental PEPT data detailing (a)-(c) Cartesian data overlayed with individual particle trajectories, (d)-(f) occupancy profiles and (g)-(i) velocity profiles for 900 g of (a),(d),(g) green, (b),(e),(h) part-roasted and (c),(f),(i) roasted coffee operated at 42 rpm, depicting the impact of roast degree. (For interpretation of the references to colour in this figure legend, the reader is referred to the web version of this article.)

as detailed in Section 2.4.4. Fig. 6(f) presents the probability density of apparent Froude number for part-roasted beans. There are clear differences. For small batch sizes, a peak at $Fr \sim 0.1$ corresponds to particles near the drum wall whose motion is driven by drum wall lifting - beans exhibit cascading motion in the transitional region ($10^{-2} < Fr < \langle 10^{-1}$). For moderate-to-large batch sizes, the distribution changes, and a peak in the range $0.2 < Fr < 0.5$ is observed; for these conditions, there is a skewed distribution of Fr, indicative of slow-moving particles further from the drum wall. For part-roasted coffee, Fig. 6(f) implies that low to moderate batch sizes (300–600 g), with low to moderate drum speeds (42–56 rpm) fall in the transitional regime between cascading and cataracting motion. Conditions corresponding to cataracting motion ($Fr > 10^{-1}$) are seen for the large batch sizes, and the transitional regimes seen here agree with previous studies of cascading to cataracting motion (Resende et al., 2017; Beaulieu et al. 2022).

In Fig. 3, the effect of roast degree (i.e., bean volume and density) on flow regimes is shown. High density (green) coffee exhibits cascading motion (Fig. 3(d)&(g)), with the dense particles falling down over the surface of the bed. As density decreases, part-roasted coffee (Fig. 3(e)&(h)) shows motion in the transitional regime between cascading and cataracting motion. For low density (roasted) coffee, cataracting motion is established (Fig. 3(f)&(i)), with roasted beans propelled much further

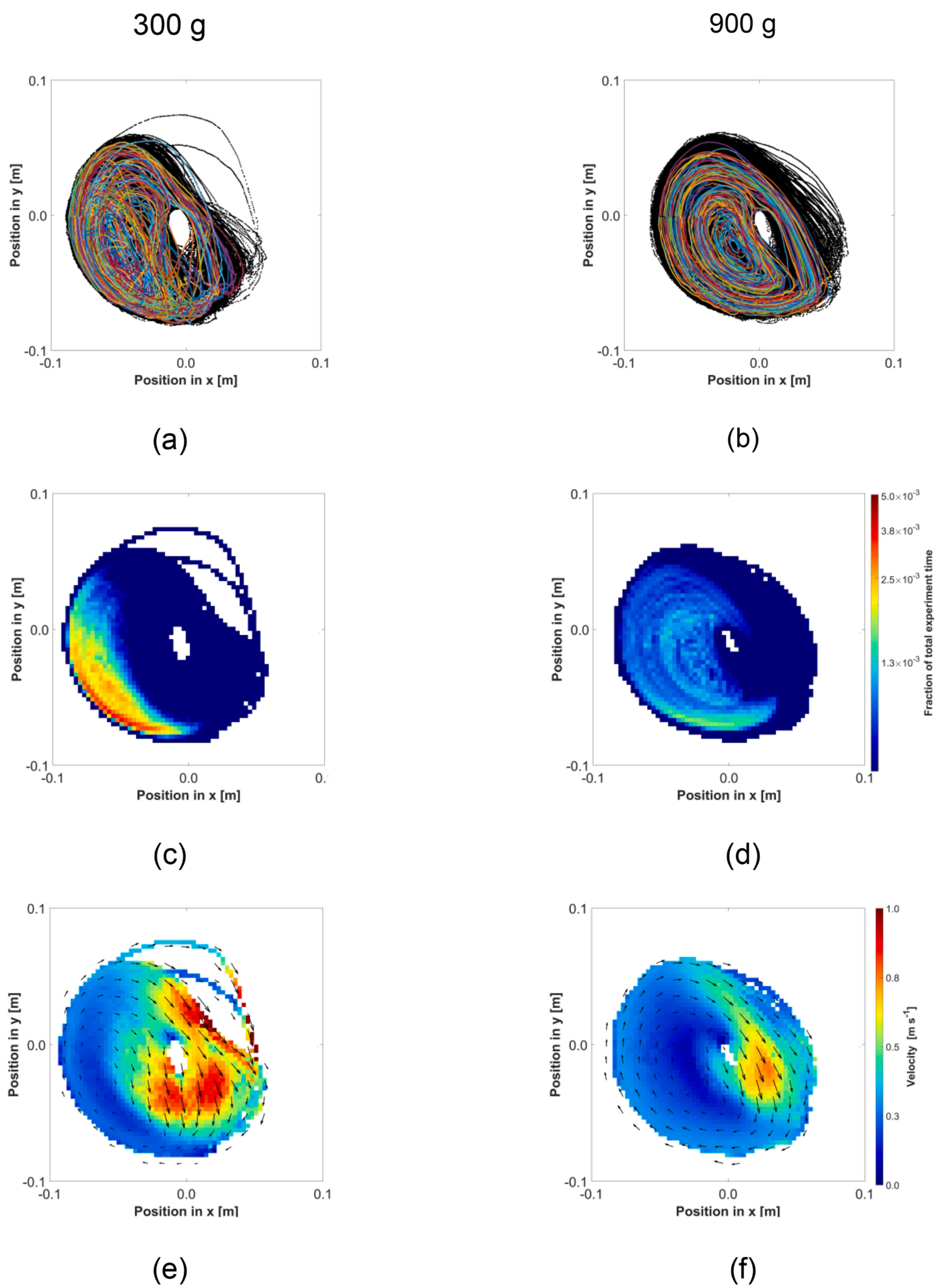

Fig. 4. Experimental PEPT data detailing (a)-(b) Cartesian data overlayed with individual particle trajectories, (c)-(d) occupancy profiles and (e)-(f) velocity profiles for (a),(c),(e) 300 g and (b),(d),(f) 900 g of roasted coffee operated at 42 rpm, depicting the impact of batch size.

and the bean bed being much smaller than for green coffee.

Volume expansion occurring between part-roasted and fully roasted stages would result in a transition in flow regime, from cascading to cataracting, during roasting. In cascading regimes, particle velocity is related to drum rotation speeds (i.e., governed by centripetal forces). In cataracting regimes ($Fr > 10^{-1}$), particles in motion at the drum wall will still be lifted, and thus governed by, the rotation speed of the drum, but in the dispersed in-flight region, particles move under gravity. Particles in these regimes are thus expected to exhibit two distinct behaviours corresponding to (i) lifting and (ii) in-flight regions.

3.4. Comparative heat transfer in rotating drum and spouted bed roasters

3.4.1. Regional heat transfer in rotating drums

For rotating drum roasters, PEPT data revealed two distinct regions of occupancy, wherein beans travel (i) slowly and have greater residence times in the bean bed and (ii) rapidly and have shorter residence times in the in-flight region (visible in Figs. 3-5). In the in-flight region, convective heat transfer is dominant, so beans will experience heat transfer governed by the convective heat transfer coefficient. Air-to-bean convective heat transfer is governed by thermophysical

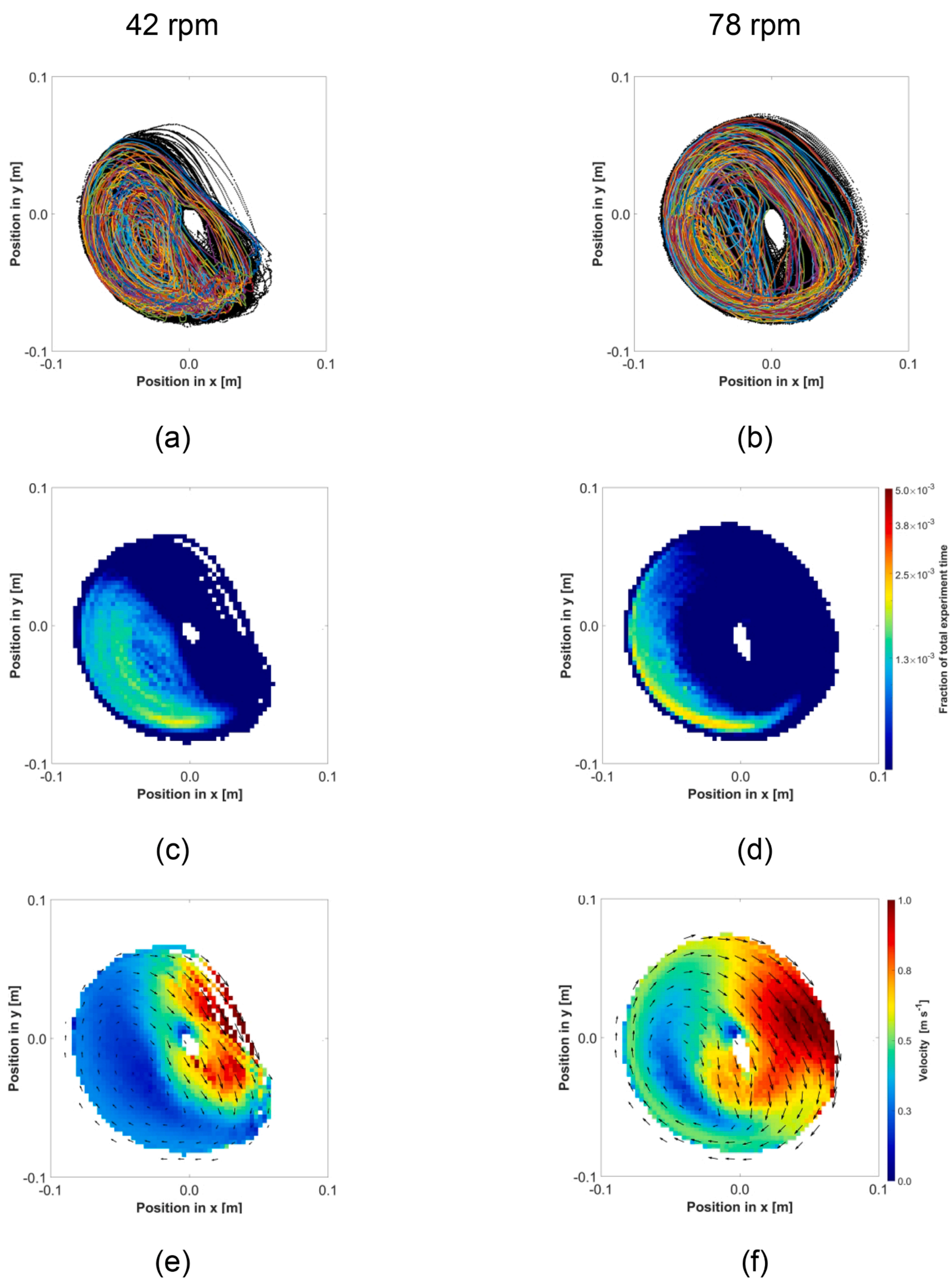

Fig. 5. Experimental PEPT data detailing (a)-(b) Cartesian data overlayed with individual particle trajectories, (c)-(d) occupancy profiles and (e)-(f) velocity profiles for 900 g of part-roasted coffee operated at (a),(c),(e) 42 rpm and (b),(d),(f) 78 rpm, depicting the impact of drum rotation speed.

properties of the roasting air (Al-Shemmeri & Lopez-Quiroga, 2022).

In the bean bed, convective heat transfer between the roasting air and individual beans will be much lower than in the in-flight region, so beans in the bulk of the bed will experience low rates of convective heat transfer. In this region, conductive heat transfer within the bean will dominate. Conductive heat transfer within the bean is governed by coffee porosity and density, which determine its thermophysical properties (i.e., thermal diffusivity, thermal conductivity and specific heat capacity) (Fabbri, Cevoli, Alessandrini, & Romani, 2011; Oliveros et al., 2017).

Beans close to the heated drum wall, particularly under conditions shown in Fig. 5(b),(d),(f), will experience rapid metal-to-bean conductive heat transfer. The drum wall is preheated to 250–300 °C, with typical steady-state charge temperatures (measured at the product thermocouple) of 180–200 °C (Garcia, Netto, Da Silva, Catão, De Souza, & Farias, 2018). When beans are close to the drum wall, metal-to-bean conductive heat transfer rates will be high, inducing rapid heating of the beans. Similar phenomena have been described for roasting of specialty malts (Robbins, 2003) where most heating occurs to particles in the wall region. Controlling the behaviour of the bed will thus be critical in roasting as changes in bean properties will affect the bed size - seen in Fig. 7(a-c) - and the induced heat transfer rate to beans in the bean bed.

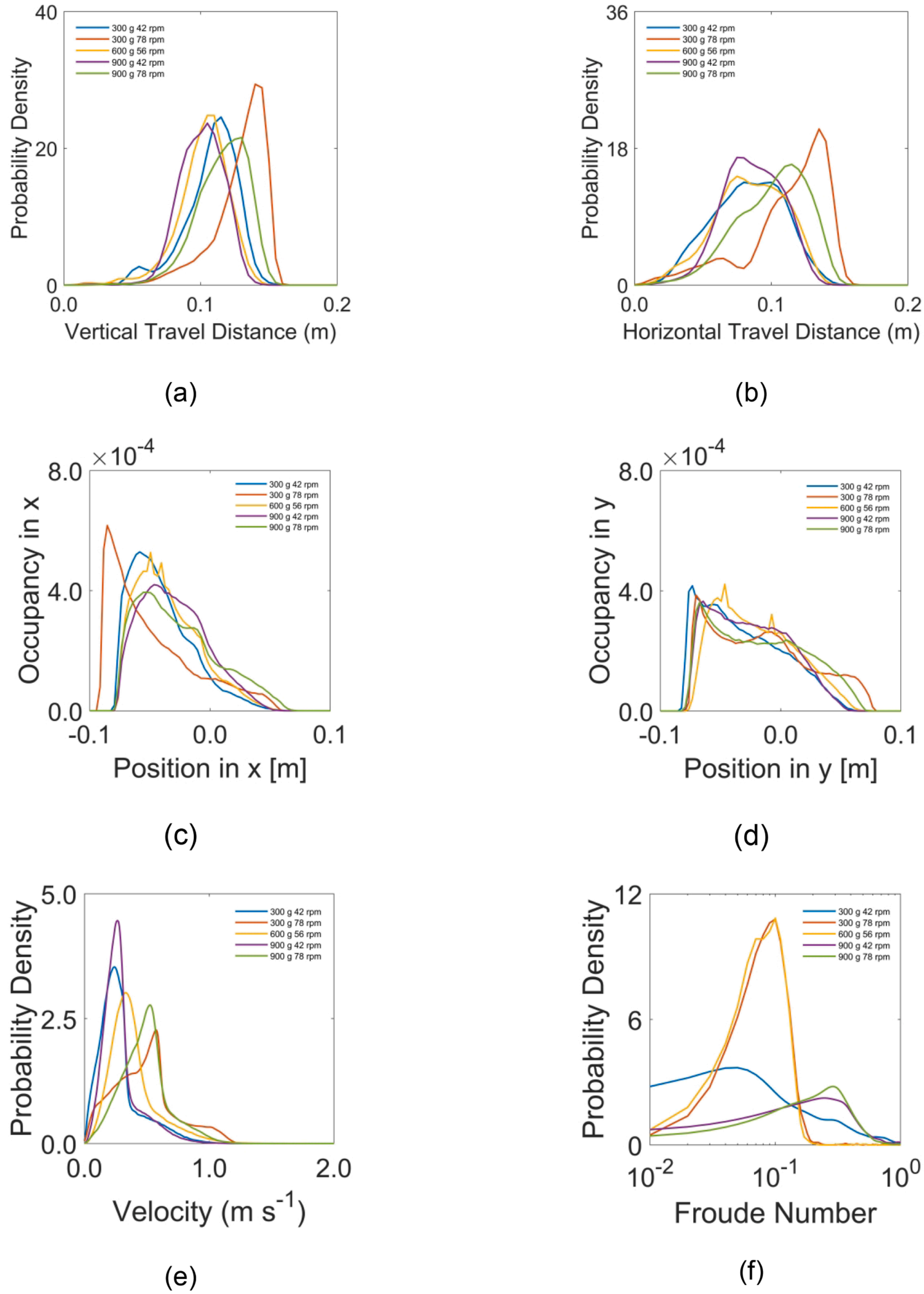

Fig. 6. Distributions of (a) vertical travel distance, (b) horizontal travel distance, (c) occupancy in *x*, (d) occupancy in *y*, (e) velocity and (f) Froude number for part-roasted coffee subject to different process conditions.

As the mapped changes in bean bed mass fraction are attributed to changes in bulk density, roaster operators can adapt their control strategy according to accessible measurements of coffee's bulk density.

3.4.2. Comparison with spouted bed roasters

Studies of coffee bean particle motion in spouted bed roasters also demonstrated two distinct regions of occupancy: (i) the dense bean bed and (ii) the dilute freeboard (Al-Shemmeri et al., 2021). Whilst similar behaviour was observed here in rotating drums (Figs. 3-5), the two systems will exhibit very different heat transfer behaviour. In spouted bed roasters, the wall is indirectly heated via convection from the roasting air (considered as heat loss) and the wall is typically at temperatures similar those of the coffee beans, so negligible wall-to-bean heat transfer is expected. Heat transfer will mostly occur in the spout region, where heated air contacts the beans. In contrast, wall-to-bean conductive heat transfer coefficient will be more important in drums.

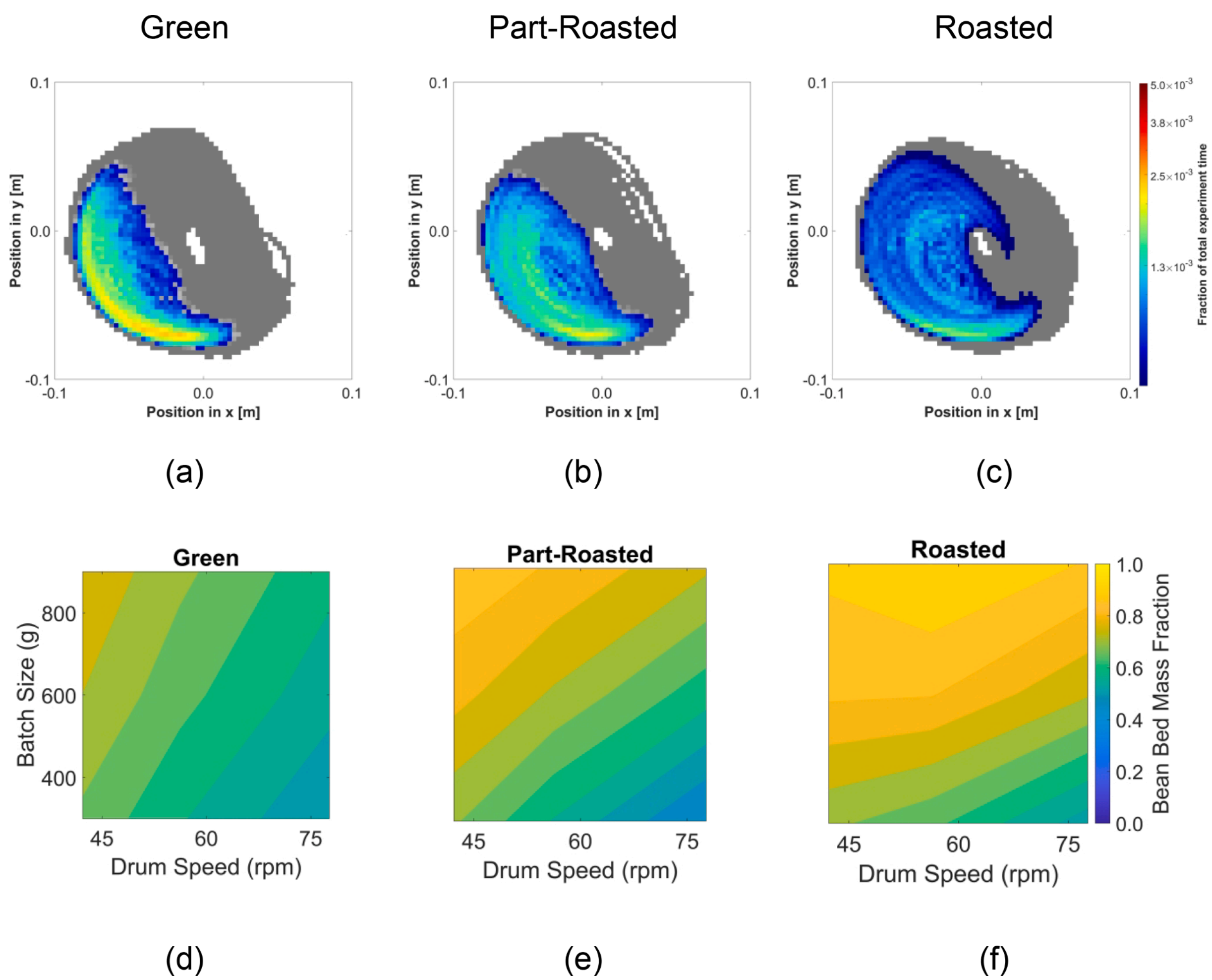

Fig. 7. Bean bed delineation – indicating bed area (in *xy*) – for 900 g of (a) green, (b) part-roasted and (c) roasted coffee operated at 42 rpm; effect of drum speed and batch size on Bean Bed Mass Fraction (BBMF) for (d) green, (e) part-roasted and (f) roasted coffee. (For interpretation of the references to colour in this figure legend, the reader is referred to the web version of this article.)

As the heat transfer conditions are different between the two roasting systems, the physical, chemical and sensorial profile of coffee roasted on each system, even under similar time–temperature histories will differ.

3.4.3. Size of bean bed

Heat transfer in the bean bed is critical. The impact of batch size, drum rotation speed and roast degree (i.e., bean density) on bean-bed mass fraction (BBMF), as given by Equation (4), is displayed in Fig. 7 (d-f). Data shown in those graphs indicate a greater influence of drum rotation speed (S_R) on BBMF in the range $56 \le S_R \le 78$ rpm than $42 \le S_R \le 56$ rpm. This is attributed to the transition from cascading to cataracting flow regimes, where $Fr \sim 10^{-1}$. For green and part-roasted coffee, greater drum rotation speeds decreased BBMF.

High rotation speeds (78 rpm) positively shift the shape of the velocity distribution (Fig. 6(e)), which is indicative of a transition in flow regime – this was also observed for large batches (900g) of part-roasted coffee when operating at high rotation speeds (78 rpm). A corresponding peak in y-axis occupancy is seen (at y = 0.01 m) in Fig. 6(d) – possibly due to collisions with the central axle. Obtained velocity data also demonstrates that increasing drum rotation speeds increase median particle velocity (v_p).

For green and part-roasted coffee (higher density), the combination of low batch sizes and high drum rotation speeds induces a slow-moving core, so that within the bean bed, particle residence times are high. This phenomenon is not observed for roasted coffee. For large batches (900 g) of roasted coffee, increasing drum rotation speed (from 42 to 78 rpm) has little influence on BBMF (Fig. 7(d-f)), but mean particle velocity increases almost two-fold (from 0.25 to 0.48 m s^{-1}). Drum rotation speeds increase (v_p) for all combinations of bean density and batch size, yet batch size (i.e., fill volume) and bean volume have little effect on (v_p), but significantly change the distribution of particle velocities as previously discussed.

Bean bed delineation depicted in Fig. 7(a-c) shows that, due to the evolution of density during roasting, the fill volume increases and reduces the area of the in-flight region. With greater drum rotation speeds, drum wall lifting affects particle trajectories significantly and for smaller batch sizes, the area of the in-flight region is maximised. Manipulation of drum speed – batch size combinations will enable roasters to modulate the dominant heat transfer mechanisms and successfully control coffee development during roasting, whilst responding to dynamic changes in product properties.

3.4.4. Outlook - best practices for rotating drum roasters

Process parameters (batch size and drum rotation speed) have been shown to strongly determine particle dynamics, for example in the different bed shapes seen in Fig. 7(a-c). Use of small batch sizes with high rotation speeds, operating in the cataracting regime where greater drum wall lifting is observed, may increase the likelihood of roast defects due to greater convective heat transfer in the in-flight region and localised conductive heat transfer near the wall, due to greater residence times in both regions. Both will decrease batch homogeneity if the time–temperature profile is not well managed. Best practice to minimise roast defects and preserve quality may involve operating near the roaster load capacity, with moderate drum rotation speeds that decrease during roasting; this protocol, combined with a well-managed time–temperature profile, would ensure maximum productivity and efficiency.

For process and product consistency, current industry practices maintain a constant batch size on a mass basis. Green coffee, the unroasted raw material, is an agricultural product with inherent natural variability, so coffee density varies not only due to post-harvest processing differences, but also within a coffee lot from a single producer. Specification of batch size on a volume basis, calculated from bulk density, would enable constant fill volumes to be achieved from batch to batch. Constant fill volume would ensure that the bean bed on a macro-scale would be of equivalent size across batches, with similar (and more predictable) particle dynamics and heat transfer conditions.

Batch homogeneity is critical for downstream processes at both factory and consumer level. Uniform coffee development can be achieved by modulating process parameters (i.e., decreasing drum rotation speed and thermal set point) as coffee properties evolve during roasting. Common roasting defects such as tipping, scorching and baking, that occur due to poorly managed roasting profiles, can also be avoided by tuning process conditions such as the preheating protocol, charge temperature and batch-to-batch protocol. PEPT has provided fundamental tools to guide roasting developers in their quest for great coffee. They can be used to virtualise the development of processes and products, improving both in-cup quality and engineering efficiency. Both the Lagrangian and Eulerian data can be used to (i) calibrate DEM simulations, (ii) generate physics-driven models to describe the transient properties of the bean bed and in-flight regions, and (iii) inform the convective boundary conditions and time-step in zero- and three-dimensional heat and mass transfer simulations. Che et al., (2023) recently outlined a framework for validation of CFD-DEM simulations using PEPT – this approach could be applied to DEM simulations of rotating drum roasters.

4. Conclusions

Using PEPT, aspherical (coffee bean) particle motion has been characterised in a real, pilot-scale rotating drum without roasting. Coffee roasting was emulated through the study of coffees with different roast degrees and densities. Translation of PEPT-captured Lagrangian trajectories to time-averaged Eulerian flow fields revealed the impact of drum rotation speed, batch size and bean density on the system particle dynamics.

Distinct regions of occupancy and velocity were identified, corresponding to (i) a disperse region of in-flight particles, with lower occupancy and higher velocities and (ii) a dense bean bed, with higher occupancy and lower velocities. From the Eulerian flow fields, regional mass fractions and median particle velocities can be obtained as a function of process parameters and product properties, to be then used with effective Froude numbers to characterise granular flow. The effect of process parameters and their variation on coffee bean particle motion in rotating drums has been also demonstrated here, revealing that process and product developers thus have two critical parameters to leverage in the pursuit of quality: batch size and drum rotation speed.

CRediT authorship contribution statement

Mark Al-Shemmeri: Investigation, Writing – original draft. **Kit Windows-Yule:** Writing – review & editing. **Estefania Lopez-Quiroga:** Formal analysis, Supervision, Writing – review & editing. **Peter J. Fryer:** Conceptualization, Writing – review & editing, Supervision, Funding acquisition.

Declaration of Competing Interest

The authors declare the following financial interests/personal relationships which may be considered as potential competing interests: Author M. Al-Shemmeri is in receipt of an EngD studentship grant supported by Jacobs Douwe Egberts and EPSRC.

Data availability

Data will be made available on request.

Acknowledgements

Authors would like to acknowledge funding from EPSRC through the Centre for Doctoral Training in Formulation Engineering (grant no. EP/L015153/1) and from Jacobs Douwe Egberts, as well as access to computational resources provided by the BlueBEAR HPC services (University of Birmingham). Authors would like also to thank the support received from Dr. Robert Farr, Modelling Expert at Jacobs Douwe Egberts, as well as Prof. Tzany Kokalova-Wheldon and the PEPT team in the School of Physics and Astronomy at Birmingham.

References

Abdul Ghani, N. H., Bingol, G., Li, B., Yu, W., & Young, B. (2019). Development of a novel 2D single coffee bean model and comparison with a 3D model under varying heating profiles. *Journal of Food Process Engineering, 42*(4). https://doi.org/10.1111/jfpe.13063

Alessandrini, L., Romani, S., Pinnavaia, G., & Rosa, M. D. (2008). Near infrared spectroscopy: An analytical tool to predict coffee roasting degree. *Analytica Chimica Acta, 625*(1), 95–102. https://doi.org/10.1016/j.aca.2008.07.013

Alonso-Torres, B., Hernández-Pérez, J. A., Sierra-Espinoza, F., Schenker, S., & Yeretzian, C. (2013). Modeling and validation of heat and mass transfer in individual coffee beans during the coffee roasting process using computational fluid dynamics (CFD). *Chimia, 67*(4), 291–294. https://doi.org/10.2533/chimia.2013.291

Al-Shemmeri, M., Windows-Yule, K., Lopez-Quiroga, E. & Fryer, P.J. (2021). Coffee bean particle motion in a spouted bed measured using Positron Emission Particle Tracking (PEPT). *Journal of Food Engineering 311*, art. no. 110709. DOI: 10.1016/j.jfoodeng.2021.110709.

Al-Shemmeri, M., E. Lopez-Quiroga & P. Fryer (2022). Simulation of coffee roasting time-temperature profiles. In Proceedings of 12th International Conference on Simulation and Modelling in the Food and Bio-Industry (FOODSIM). Ghent (Belgium). EUROSIS-ETI.

Alstrup, J., Petersen, M. A., Larsen, F. H., & Münchow, M. (2020). The effect of roast development time modulations on the sensory profile and chemical composition of the coffee brew as measured by NMR and DHS-GC-MS. *Beverages, 6*(4), 1–14. https://doi.org/10.3390/beverages6040070

Arntz, M. M. H. D., Den Otter, W. K., Briels, W. J., Bussmann, P. J. T., Beeltink, H. H., & Boom, R. M. (2008). Granular mixing and segregation in a horizontal rotating drum: A simulation study on the impact of rotational speed and fill level. *AIChE Journal, 54*(12), 3133–3146. https://doi.org/10.1002/aic.11622

Azmir, J., Hou, Q., & Yu, A. (2020). CFD-DEM study of the effects of food grain properties on drying and shrinkage in a fluidised bed. *Powder Technology, 360*, 33–42. https://doi.org/10.1016/j.powtec.2019.10.021

Beaulieu, C., Vidal, D., Niyonkuru, C., Wachs, A., Chaouki, J., & Bertrand, F. (2022). Effect of particle angularity on flow regime transitions and segregation of bidisperse blends in a rotating drum. *Computational Particle Mechanics, 9*(3), 443–463. https://doi.org/10.1007/s40571-021-00421-1

Brown, S. L., & Lattimer, B. Y. (2013). Transient gas-to-particle heat transfer measurements in a spouted bed. *Experimental Thermal and Fluid Science, 44*, 883–892. https://doi.org/10.1016/j.expthermflusci.2012.10.004

Bruchmüller, J., Gu, S., Luo, K. H., & Van Wachem, B. G. M. (2010). Discrete element method for multiscale modeling. *Journal of Multiscale Modeling, 2*(1–2), 147–162. https://doi.org/10.1142/S1756973710000254

Che, H., Al-Shemmeri, M., Fryer, P., Lopez-Quiroga, E., Kokalova Wheldon, T., & Windows-Yule, K. (2023). PEPT validated CFD-DEM model of aspherical particle motion in a spouted bed. *Chemical Engineering Journal, 453*(1). https://doi.org/10.1016/j.cej.2022.139689

Chiang, C., Wu, D., & Kang, D. (2017). Detailed simulation of fluid dynamics and heat transfer in coffee bean roaster. *Journal of Food Process Engineering, 40*(2). https://doi.org/10.1111/jfpe.12398

Cristo, H. P., Martins, M. A., Oliveira, L. S., & Franca, A. S. (2006). Transverse flow of coffee beans in rotating roasters. *Journal of Food Engineering, 75*(1), 142–148. https://doi.org/10.1016/j.jfoodeng.2005.04.010

Ding, Y. L., Forster, R., Seville, J. P. K., & Parker, D. J. (2002). Segregation of granular flow in the transverse plane of a rolling mode rotating drum. *International Journal of Multiphase Flow, 28*(4), 635–663. https://doi.org/10.1016/S0301-9322(01)00081-7

Fabbri, A., Cevoli, C., Alessandrini, L., & Romani, S. (2011). Numerical modeling of heat and mass transfer during coffee roasting process. *Journal of Food Engineering, 105*(2), 264–269. https://doi.org/10.1016/j.jfoodeng.2011.02.030

Gancarz, M., Dobrzański, B., Malaga-Toboła, U., Tabor, S., Combrzyński, M., Ćwikła, D., Strobel, W., Oniszczuk, A., Karami, H., Darvishi, Y., Żytek, A., & Rusinek, R. (2022). Impact of Coffee Bean Roasting on the Content of Pyridines Determined by Analysis of Volatile Organic Compounds. *Molecules, 27*(5). https://doi.org/10.3390/molecules27051559

Garcia, C. C., Netto, A. D. P., Da Silva, M. C., Catão, A. A., De Souza, I. A., Farias, L. S., . . . Da Silva Junior, A. I. (2018). Relative importance and interaction of roasting variables in coffee roasting process. [Importância relativa e interação das variáveis de torra no processo de torrefação de café] *Coffee Science, 13*(3), 379-388. DOI: https://doi.org/10.25186/cs.v13i3.1483.

Giacalone, D., Degn, T. K., Yang, N., Liu, C., Fisk, I., & Münchow, M. (2019). Common roasting defects in coffee: Aroma composition, sensory characterization and consumer perception. *Food Quality and Preference., 71*, 463–474. https://doi.org/10.1016/j.foodqual.2018.03.009

González, S., Windows-Yule, C. R. K., Luding, S., Parker, D. J., & Thornton, A. R. (2015). Forced axial segregation in axially inhomogeneous rotating systems. *Physical Review E - Statistical, Nonlinear, and Soft Matter Physics, 92*(2). https://doi.org/10.1103/PhysRevE.92.022202

Govender, I. (2016). Granular flows in rotating drums: A rheological perspective. *Minerals Engineering, 92*, 168–175. https://doi.org/10.1016/j.mineng.2016.03.021

Henein, H., Brimacombe, J. K., & Watkinson, A. P. (1983). Experimental study of transverse bed motion in rotary kilns. *Metallurgical Transactions B, 14*(2), 191–205. https://doi.org/10.1007/BF02661016

Herald, M., Wheldon, T., & Windows-Yule, C. (2021). MonteCarlo model validation of a detector system used for positron emission particle tracking. *Nuclear Instruments and Methods in Physics Research, Section A: Accelerators, Spectrometers, Detectors and Associated Equipment, 993*. https://doi.org/10.1016/j.nima.2021.165073

Hoos, R. (2015). *Modulating the flavour profile of coffee*. Portland (OR), USA: Hoos Coffee Consulting.

Ingram, A., Seville, J., Parker, D., Fan, X., & Forster, R. (2005). Axial and radial dispersion in rolling mode rotating drums. *Powder Technology, 158*(1–3), 76–91. https://doi.org/10.1016/j.powtec.2005.04.030

Jones, C. R., Corona, A., Amador, C., & Fryer, P. J. (2021). Dynamics of fabric and dryer sheet motion in domestic clothes dryers. *Drying Technology, 40*(10), 2087–2104. https://doi.org/10.1080/07373937.2021.1918706

Juarez, G., Chen, P., & Lueptow, R. M. (2011). Transition to centrifuging granular flow in rotating tumblers: A modified Froude number. *New Journal of Physics, 13*. https://doi.org/10.1088/1367-2630/13/5/053055

Lim, S., Davidson, J. F., Forster, R. N., Parker, D. J., Scott, D. M., & Seville, J. P. K. (2003). Avalanching of granular material in a horizontal slowly rotating cylinder: PEPT studies. *Powder Technology, 138*(1), 25–30. https://doi.org/10.1016/j.powtec.2003.08.038

Ma, H., Zhou, L., Liu, Z., Chen, M., Xia, X., Zhao, Y. (2022) A review of recent development for the CFD-DEM investigations of non-spherical particles. *Powder Technology*, *412*. DOI: https://doi.org/10.1016/j.powtec.2022.117972.

Machado, M., I. Resende, R. Lima, R. Brandão, M. Pivello, S. Nascimento, C. Duarte and M. Barrozo (2018). The role of boundary conditions on the dynamics of green coffee beans in a rotated dryer. In Proceedings of the 21st International Drying Symposium IDS 2018. Valencia (Spain). Editorial Universitat Politècnica de València.

Mellmann, J. (2001). The transverse motion of solids in rotating cylinders-forms of motion and transition behavior. *Powder Technology, 118*(3), 251–270. https://doi.org/10.1016/S0032-5910(00)00402-2

Morrison, A. J., Govender, I., Mainza, A. N., & Parker, D. J. (2016). The shape and behaviour of a granular bed in a rotating drum using Eulerian flow fields obtained from PEPT. *Chemical Engineering Science, 152*, 186–198. https://doi.org/10.1016/j.ces.2016.06.022

Münchow, M., Alstrup, J., Steen, I., & Giacalone, D. (2020). Roasting conditions and coffee flavor: A multi-study empirical investigation. *Beverages, 6*(2), 1–14. https://doi.org/10.3390/beverages6020029

Nicuşan, A. L., & Windows-Yule, C. R. K. (2020). Positron emission particle tracking using machine learning. *Review of Scientific Instruments, 91*(1). https://doi.org/10.1063/1.5129251

Oliveros, N. O., Hernández, J. A., Sierra-Espinosa, F. Z., Guardián-Tapia, R., & Pliego-Solórzano, R. (2017). Experimental study of dynamic porosity and its effects on simulation of the coffee beans roasting. *Journal of Food Engineering, 199*, 100–112. https://doi.org/10.1016/j.jfoodeng.2016.12.012

Otsu, N. (1979). Threshold selection method from gray-level histograms. *IEEE Transactions of Systems, Man and Cybernetics, SMC-9(1)*, 62–66. https://doi.org/10.1109/tsmc.1979.4310076

Parker, D. J. (2017). Positron emission particle tracking and its application to granular media. *Review of Scientific Instruments, 88*(5). https://doi.org/10.1063/1.4983046

Parker, D. J., Broadbent, C. J., Fowles, P., Hawkesworth, M. R., & McNeil, P. (1993). Positron emission particle tracking - a technique for studying flow within engineering equipment. *Nuclear Instruments and Methods in Physics Research, A, 326* (3), 592–607. https://doi.org/10.1016/0168-9002(93)90864-E

Parker, D., Forster, R., Fowles, P., & Takhar, P. (2002). Positron emission particle tracking using the new Birmingham positron camera. *Nuclear Instruments and Methods in Physics Research Section A: Accelerators, Spectrometers, Detectors and Associated Equipment, 477*(1), 540–545. https://doi.org/10.1016/S0168-9002(01)01919-2

Pathmathas, T. (2015). *Granular flow modelling of rotating drum flows using positron emission particle tracking*. University of Cape Town (South Africa).

Pittia, P., Dalla Rosa, M., & Lerici, C. R. (2001). Textural changes of coffee beans as affected by roasting conditions. *LWT, 34*(3), 168–175. https://doi.org/10.1006/fstl.2000.0749

Rao, S. (2020). *Coffee Roasting - Best Practices (1st Edition)*. ISBN: 9781792327759. Canada.

Resende, I. A., Machado, M. V. C., Duarte, C. R., & Barrozo, M. A. S. (2017). An experimental analysis of coffee beans dynamics in a rotary drum. *Canadian Journal of Chemical Engineering, 95*(12), 2239–2248. https://doi.org/10.1002/cjce.22961

Robbins, P. T. (2003). *The roasting of speciality malts*. University of Birmingham (UK).

Romani, S., Cevoli, C., Fabbri, A., Alessandrini, L., & Dalla Rosa, M. (2012). Evaluation of coffee roasting degree by using electronic nose and artificial neural network for off-line quality control. *Journal of Food Science, 77*(9), C960–C965. https://doi.org/10.1111/j.1750-3841.2012.02851.x

Schenker, S., & Rothgeb, T. (2017). The roast - creating the beans' signature. In B. Folmer (Ed.), *The craft & science of coffee* (pp. 245–271). Academic Press. https://doi.org/10.1016/B978-0-12-803520-7.00011-6.

Wildman, R. D., Huntley, J. M., Hansen, J., & -., Parker, D. J., & Allen, D. A.. (2000). Single-particle motion in three-dimensional vibrofluidized granular beds. *Physical Review E - Statistical Physics, Plasmas, Fluids, and Related Interdisciplinary Topics, 62*(3 B), 3826–3835. https://doi.org/10.1103/PhysRevE.62.3826

Windows-Yule, K., L. Nicuşan, M. T. Herald, S. Manger and D. Parker (2022b). Positron Emission Particle Tracking. A comprehensive guide. IOP Publishing Ltd. (London, UK). DOI: https://doi.org/10.1088/978-0-7503-3071-8.

Windows-Yule, C. R. K., Herald, M. T., Nicuşan, A. L., Wiggins, C. S., Pratx, G., Manger, S., … Parker, D. J. (2022a). *Recent advances in positron emission particle tracking: A comparative review, 85*. https://doi.org/10.1088/1361-6633/ac3c4c

Windows-Yule, C. R. K., Scheper, B. J., Horn, A. J. V. D., Hainsworth, N., Saunders, J., Parker, D. J., & Thornton, A. R. (2016). Understanding and exploiting competing segregation mechanisms in horizontally rotated granular media. *New Journal of Physics, 18*(2). https://doi.org/10.1088/1367-2630/18/2/023013

Windows-Yule, C. R. K., Seville, J. P. K., Ingram, A., & Parker, D. J. (2020). Positron emission particle tracking of granular flows. *Annual Review of Chemical and Biomolecular Engineering, 11*, 367–396. https://doi.org/10.1146/annurev-chembioeng-011620-120633

Windows-Yule, C. R. K., Van Der Horn, A. J., Tunuguntla, D. R., Parker, D. J., & Thornton, A. R. (2017). Inducing axial banding in bidisperse-by-density granular systems using noncylindrical tumbler geometries. *Physical Review Applied, 8*(2). https://doi.org/10.1103/PhysRevApplied.8.024010